Supporting Information

for

Activity of N-H in Phenothiazine Derivatives: Synthesis and Applications in Fluoride Ions Sensing and Electrochromism

Weidong Zhang,[a] Xiucun Feng,[a] Chao Zhang,[a] Qiangqiang Jia,[d] Xingliang Liu*[a] and Kun Zhou*[b,c]*

[a] School of Chemical Engineering, Qinghai University, Xining, 810016, China
E-mail: zhangwd@qhu.edu.cn
[b] *School of Science and Engineering, Shenzhen Institute of Aggregate Science and Technology, The Chinese University of Hong Kong, Shenzhen, Guangdong 518172, China.*
E-mail: zhoukun@cuhk.edu.cn
[c] Guangdong Provincial Key Laboratory of Luminescence from Molecular Aggregates (South China University of Technology), Guangzhou 510640, China
[d] State Key Laboratory of Plateau Ecology and Agriculture, Qinghai University, Xining, 810016, China

Contents

1. The excitation and emission spectra

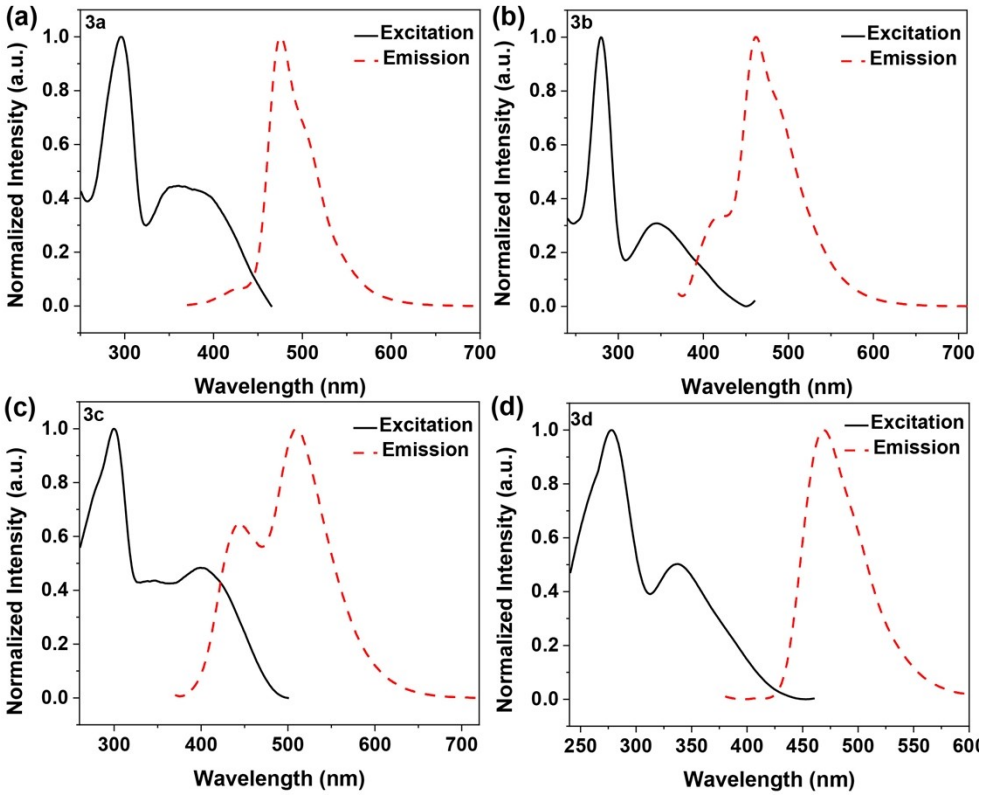

Figure S1. Fluorescence excitation (solid line) and emission spectra (dashed line) of **3a-d**.

2. The fluorescence lifetime decay spectra

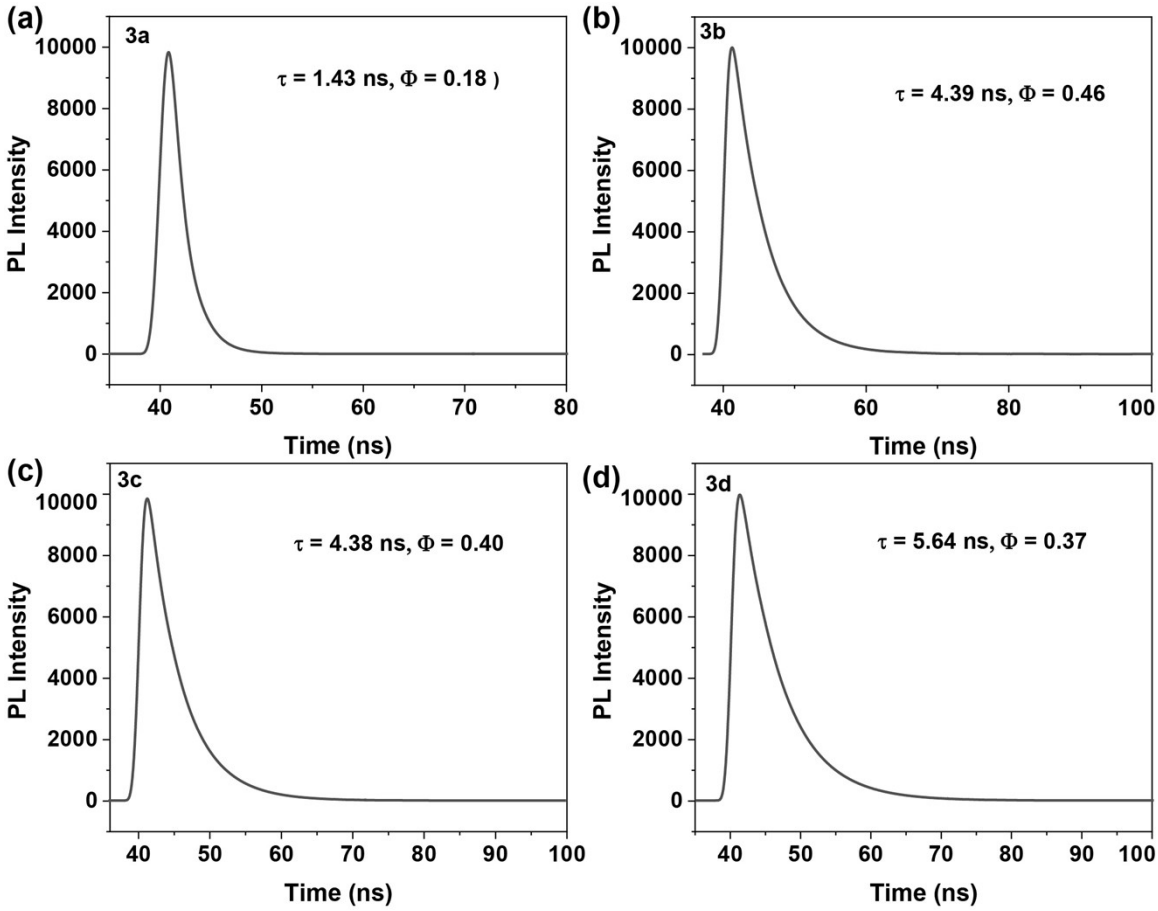

Figure S2. Fluorescence lifetime decay spectra of **3a-d**.

3. The Calculated UV-Vis spectra

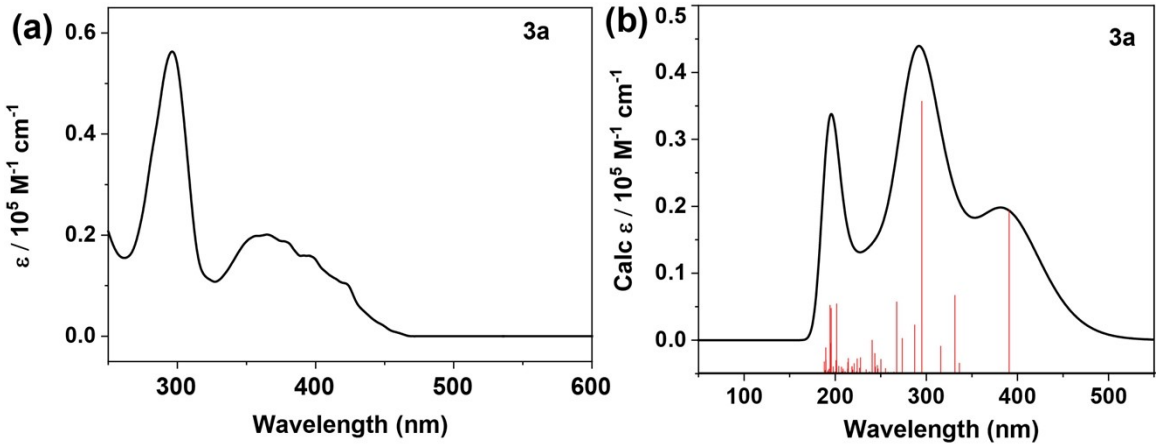

Figure S3. Computed, at the TD-DFT, B3LYP-D3/6-311g(d,p),[1-4] level of theory and experimental UV-vis spectra of **3a**.

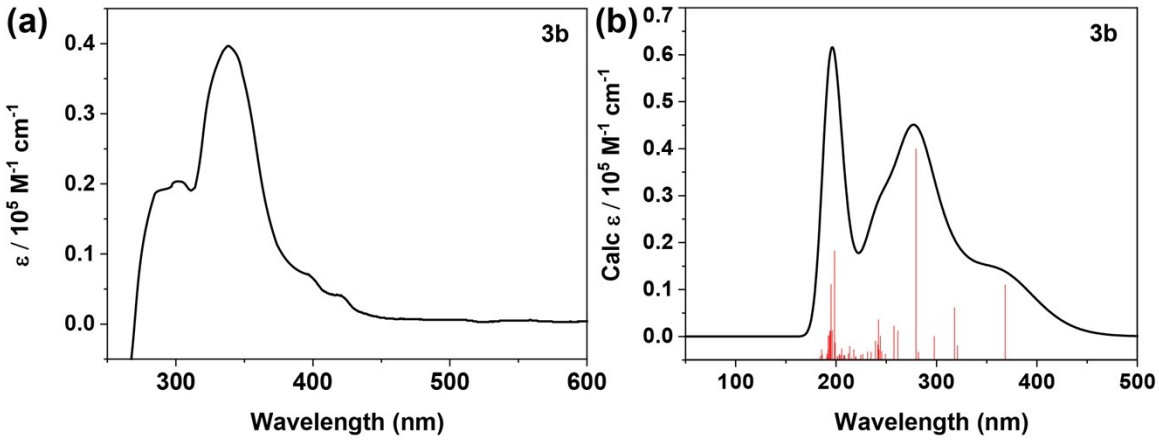

Figure S4. Computed, at the TD-DFT, B3LYP-D3/6-311g(d,p), level of theory and experimental UV-vis spectra of **3b**.

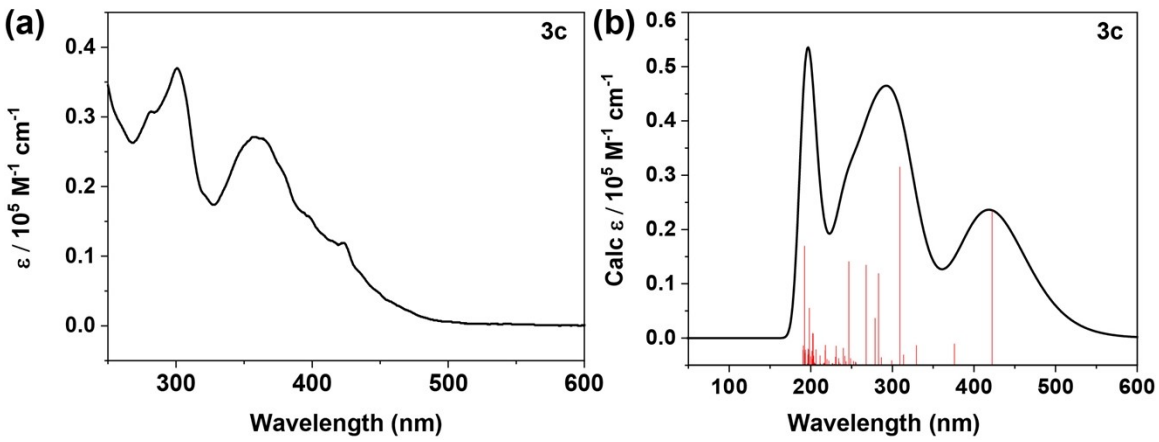

Figure S5. Computed, at the TD-DFT, B3LYP-D3/6-311g(d,p), level of theory and experimental UV-vis spectra of **3c**.

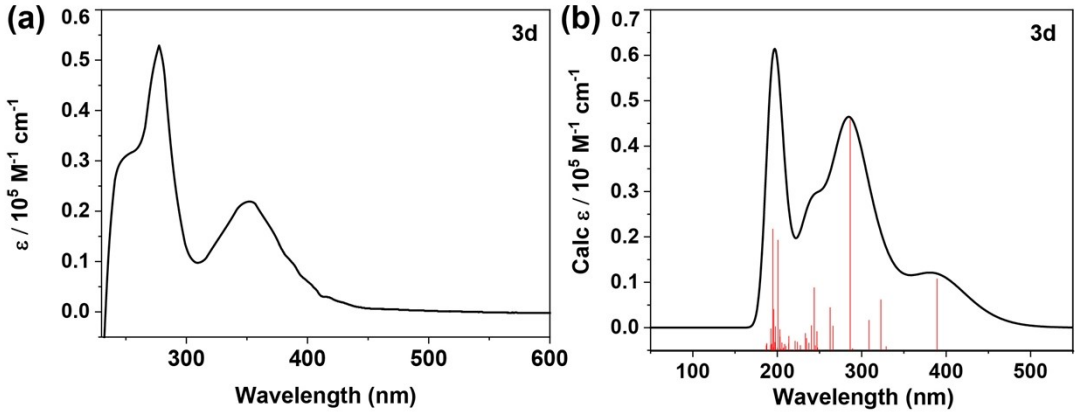

Figure S6. Computed, at the TD-DFT, B3LYP-D3/6-311g(d,p), level of theory and experimental UV-vis spectra of **3d**.

Table S1. Calculated ($\lambda_{TD\text{-}DFT}$) wavelengths of **3a**. Molecular orbitals (MOs) involved in the main electronic transition，f corresponds to the oscillator strength. (TD-DFT, B3LYP-D3/6-311g(d,p))

$\lambda_{TD\text{-}DFT}$	Oscillator Strength, f	MOs	
389.65 nm	0.4457	HOMO -> LUMO	96.18%
330.10 nm	0.2127	HOMO-2 -> LUMO	3.34%
		HOMO -> LUMO+2	92.24%
314.56 nm	0.0731	HOMO -> LUMO+1	13.27%
		HOMO -> LUMO+3	82.66%
293.82 nm	0.7451	HOMO-2 -> LUMO	81.79%
		HOMO-2 -> LUMO+2	2.03%
		HOMO-1 -> LUMO+3	2.37%
		HOMO -> LUMO+2	2.18%
		HOMO -> LUMO+4	6.01%
286.09 nm	0.1315	HOMO-1 -> LUMO	94.74
272.25 nm	0.0948	HOMO-2 -> LUMO	7.56
		HOMO-1 -> LUMO+1	2.85
		HOMO -> LUMO+4	75.93%
		HOMO ->LUMO+6	6.76
266.28 nm	0.1948	HOMO-1 -> LUMO+1	86.80%
		HOMO-1 -> LUMO+3	6.55%
242.35 nm	0.0532	HOMO-5 -> LUMO+1	4.59%
		HOMO-4 -> LUMO	61.52%
		HOMO-1 ->LUMO+7	2.07%

Table S2. Calculated ($\lambda_{TD\text{-}DFT}$) wavelengths of **3b**. Molecular orbitals (MOs) involved in the main electronic transition，f corresponds to the oscillator strength. (TD-DFT, B3LYP-D3/6-311g(d,p))

$\lambda_{TD\text{-}DFT}$	Oscillator Strength, f	MOs	
370.60 nm	0.3756	HOMO -> LUMO	96.21%
322.98 nm	0.0651	HOMO -> LUMO+1	77.00%
		HOMO -> LUMO+3	17.18%
319.34 nm	0.2786	HOMO-1 -> LUMO	2.18%
		HOMO -> LUMO+1	2.89%
		HOMO -> LUMO+2	89.73%
299.68 nm	0.1478	HOMO -> LUMO+1	17.35%
		HOMO -> LUMO+3	78.33%
282.48 nm	0.2460	HOMO-1 -> LUMO	14.41%
		HOMO -> LUMO+4	76.82%
		HOMO -> LUMO+6	2.76%
282.30 nm	0.2178	HOMO-1 -> LUMO	23.49
		HOMO -> LUMO+4	6.95%
		HOMO -> LUMO+5	60.27%

Table S3. Calculated ($\lambda_{TD\text{-}DFT}$) wavelengths of **3c**. Molecular orbitals (MOs) involved in the main electronic transition，f corresponds to the oscillator strength. (TD-DFT, B3LYP-D3/6-311g(d,p))

$\lambda_{TD\text{-}DFT}$	Oscillator Strength, f	MOs	
426.23 nm	0.6527	HOMO ->LUMO	97.74%
379.50 nm	0.1045	HOMO ->LUMO+1	98.67%
329.69 nm	0.1031	HOMO-1 ->LUMO	4.10%
		HOMO ->LUMO+2	71.64%
		HOMO ->LUMO+4	20.66%
314.95 nm	0.0598	HOMO-1 ->LUMO+1	2.74
		HOMO ->LUMO+3	71.88%
		HOMO ->LUMO+5	20.32%
310.83 nm	0.8139	HOMO-1 ->LUMO	86.31%
		HOMO ->LUMO+2	2.39%
		HOMO ->LUMO+6	3.93%

Table S4. Calculated ($\lambda_{TD\text{-}DFT}$) wavelengths of **3d**. Molecular orbitals (MOs) involved in the main electronic transition，f corresponds to the oscillator strength. (TD-DFT, B3LYP-D3/6-311g(d,p))

$\lambda_{TD\text{-}DFT}$	Oscillator Strength, f	MOs	
390.79 nm	0.3537	HOMO ->LUMO	96.74%
323.18 nm	0.2784	HOMO-1 ->LUMO	3.02%
		HOMO ->LUMO+3	91.83%
		HOMO ->LUMO+5	2.13%
309.70 nm	0.1832	HOMO ->LUMO+1	21.81
		HOMO ->LUMO+2	75.91%
288.63 nm	0.4155	HOMO-1 ->LUMO	24.13%
		HOMO ->LUMO+5	66.65
		HOMO ->LUMO+6	3.76%

4. Electrochemical properties

Cyclic voltammograms were recorded with a Metrohm PGSTAT204 electrochemical analyzer using DMF. The CV cell consisted of a gold electrode, a Pt wire counter electrode, and an Ag/AgCl reference electrode. All measurements were performed using DMF solutions of samples with a concentration of 1 mM and 0.1 M $Bu_4N^+BF_6^-$ as a supporting electrolyte with a scan rate of 100 mVs^{-1}. Potentials are determined against a ferrocene/ferrocenyl ion couple (Fc/Fc^+).

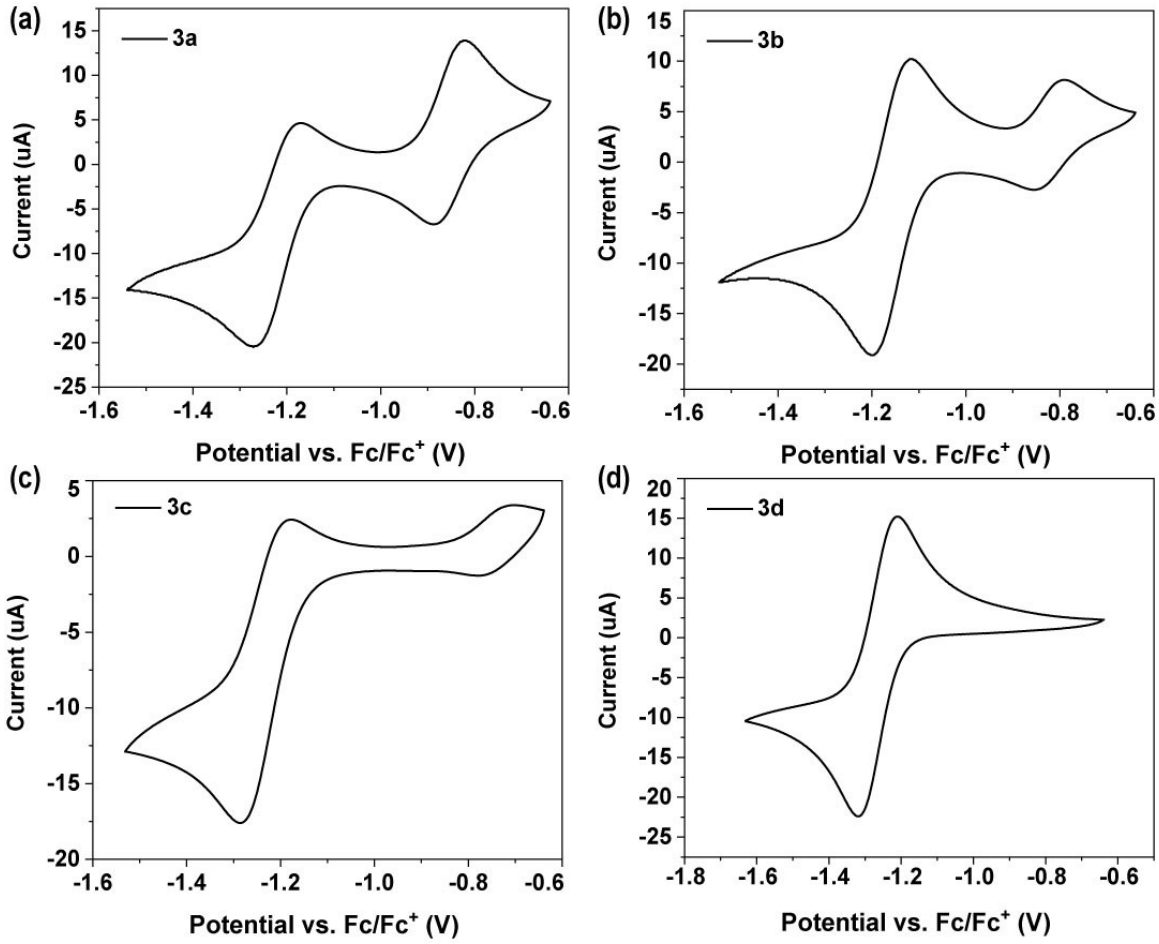

Figure S7. Cyclic voltammograms of **3a**, **3b**, **3c** and **3d** in DMF with $Bu_4N^+BF_6^-$ (0.1 M) as a supporting electrolyte, Fc = ferrocene.

5. Comparison of HOMO/LUMO plots

Table S5 Electronic properties of **3a**, **3b**, **3c** and **3d**

Entry	E_g[a](eV)	E_{red}[b](V)	LUMO(eV) (Exp)[c]	HOMO(eV) (Exp)[d]	LUMO(eV) (Cal)[e]	HOMO(eV) (Cal)[e]	E_g(eV) (Cal)[e]
3a	2.86	-1.15	-3.65	-6.51	-1.15	-4.90	3.75
3b	2.98	-1.08	-3.72	-6.70	-0.93	-4.94	4.01
3c	2.81	-1.16	-3.64	-6.45	-1.90	-5.46	3.56
3d	2.99,	-1.20	-3.60	-6.59	-0.84	-5.01	4.17

[a] E_g estimated from the UV-Vis absorption spectra.

[b] Reduction potential measured by cyclic voltammetry.

[c] LUMO = -(E_{red} + 4.8) eV.

[d] HOMO = LUMO - E_g.

[e]Theoretical calculations have been carried out by using the GAUSSIAN09 suite of programs in gas-phase at the B3LYP/6-31G(d) levele,[5] respectively.

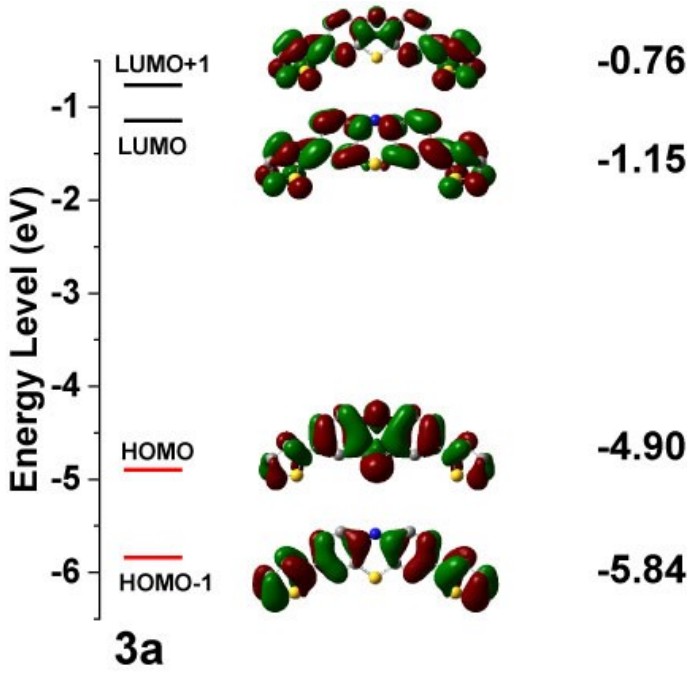

Figure S8. Computed molecular orbital plots for **3a**.

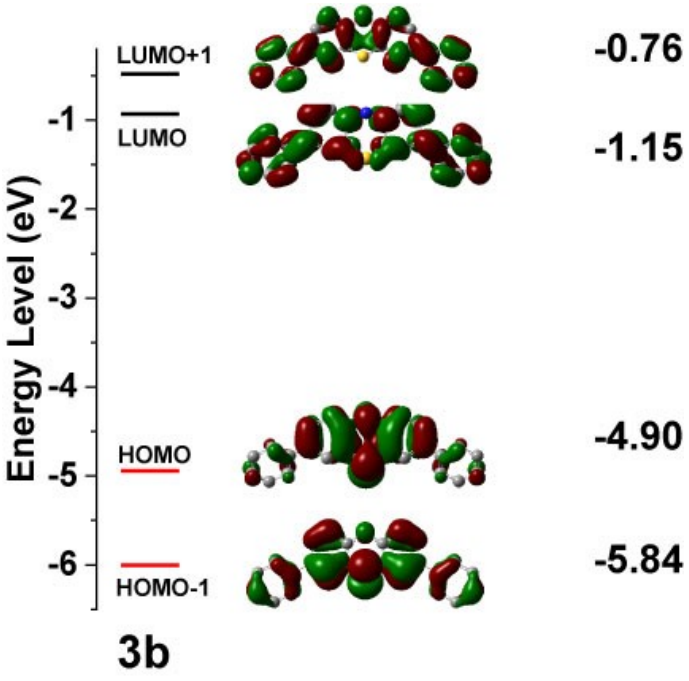

Figure S9. Computed molecular orbital plots for **3b**.

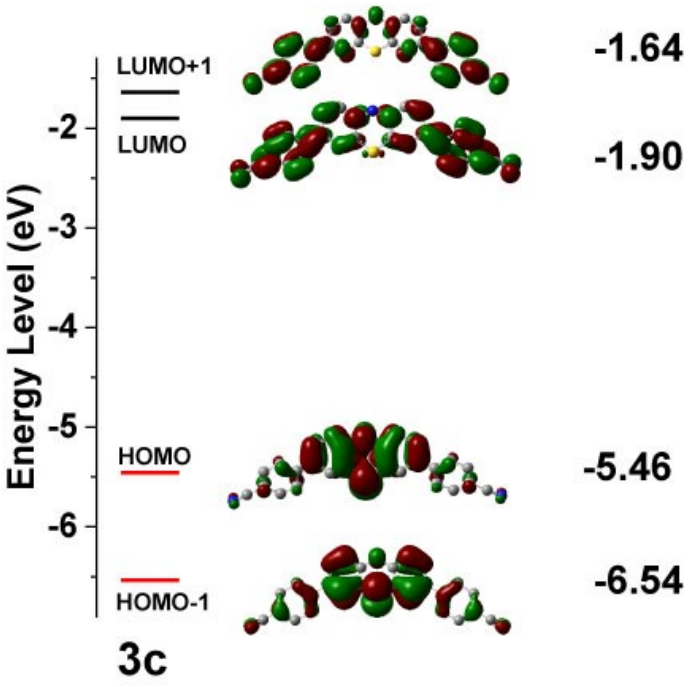

Figure S10 Computed molecular orbital plots for **3c**.

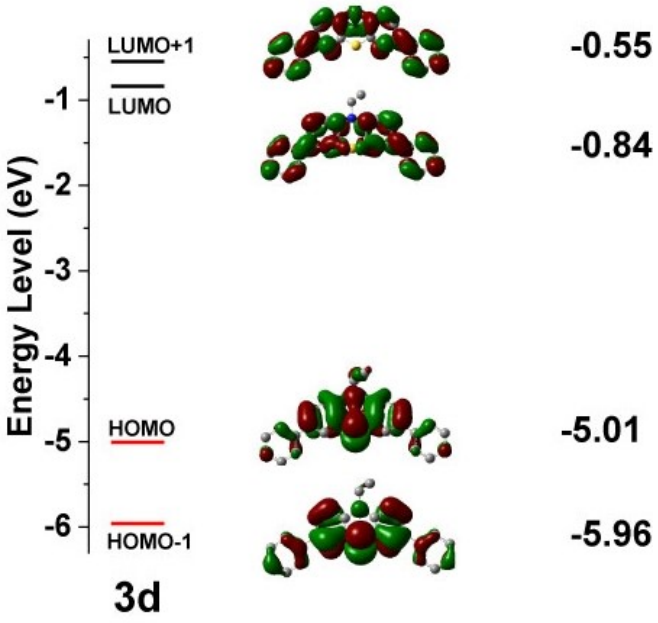

Figure S11 Computed molecular orbital plots for **3d**.

6. Fluoride titration experiments

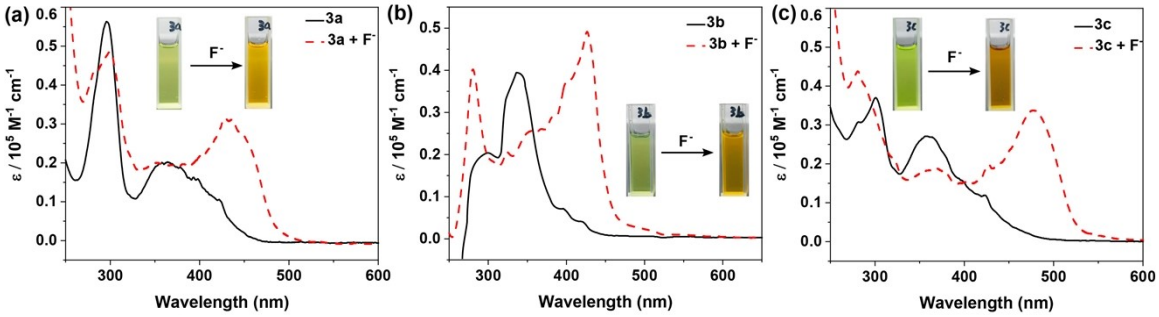

Figure S12. UV-Vis absorption spectral and solution colors of **3a-3c** changes after the addition of TBAF.

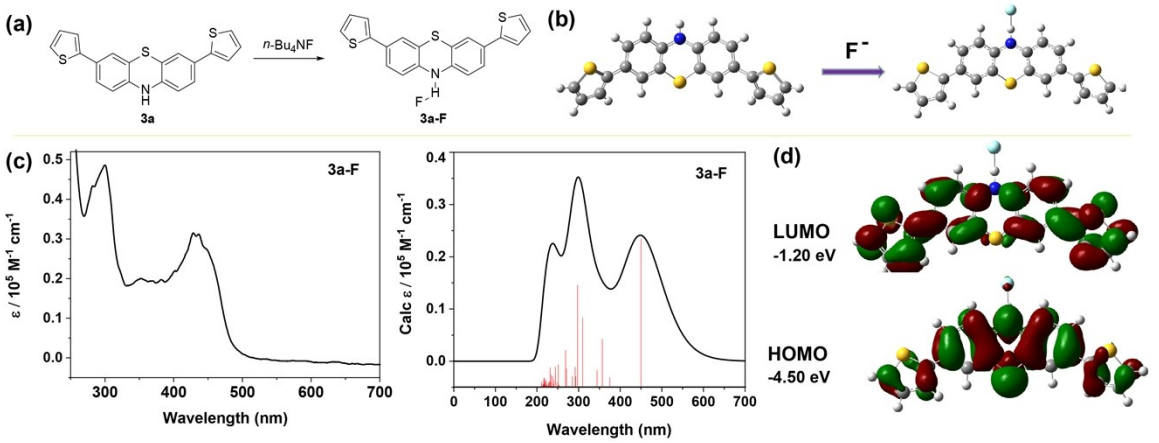

Figure S13. (a) Proposed interaction of **3a** with F^-; (b) Proposed shape changes for **3a** combined with F^-; (c) Experimental and calculated UV-Vis spectra of **3a-F** at the TD-DFT, B3LYP-D3/6-311+g(d,p) level of theory. (d) HOMO/LUMO orbital plots of **3a-F**.

Table S6. Calculated ($\lambda_{TD\text{-}DFT}$) wavelengths of **3a-F**. Molecular orbitals (MOs) involved in the main electronic transition，f corresponds to the oscillator strength. (TD-DFT, B3LYP-D3/6-311+g(d,p))

$\lambda_{TD\text{-}DFT}$	Oscillator Strength, f	MOs	
451.37 nm	0.5801	HOMO ->LUMO	96.85%
358.33 nm	0.1872	HOMO ->LUMO+3	93.85%
345.74 nm	0.0651	HOMO ->LUMO+1	6.52%
		HOMO ->LUMO+2	90.86%
311.10 nm	0.2715	HOMO-2 ->LUMO	39.69%
		HOMO-1 ->LUMO	2.68%
		HOMO ->LUMO+4	46.38%
298.92 nm	0.3986	HOMO-2 ->LUMO	42.02%
		HOMO-1 ->LUMO	7.86%
		HOMO ->LUMO+4	37.21%
		HOMO ->LUMO+5	3.45%
293.08 nm	0.3986	HOMO-2 ->LUMO	7.29%
		HOMO-1 ->LUMO	71.94%
		HOMO ->LUMO+5	14.36%
272.38 nm	0.0716	HOMO-2 ->LUMO+1	45.63%
		HOMO-1 ->LUMO+1	42.12%
		HOMO-1 ->LUMO+3	2.35%
		HOMO ->LUMO+7	2.14%
270.19 nm	0.1435	HOMO-2 ->LUMO+1	43.62%
		HOMO-1 ->LUMO+1	47.36%
		HOMO-1 ->LUMO+2	2.66%
245.79 nm	0.0783	HOMO-5 ->LUMO	10.02%
		HOMO-3 ->LUMO	7.59%
		HOMO-2 ->LUMO+3	15.71%
		HOMO-1 ->LUMO+2	9.78%
		HOMO ->LUMO+12	3.58%
		HOMO ->LUMO+14	40.14%

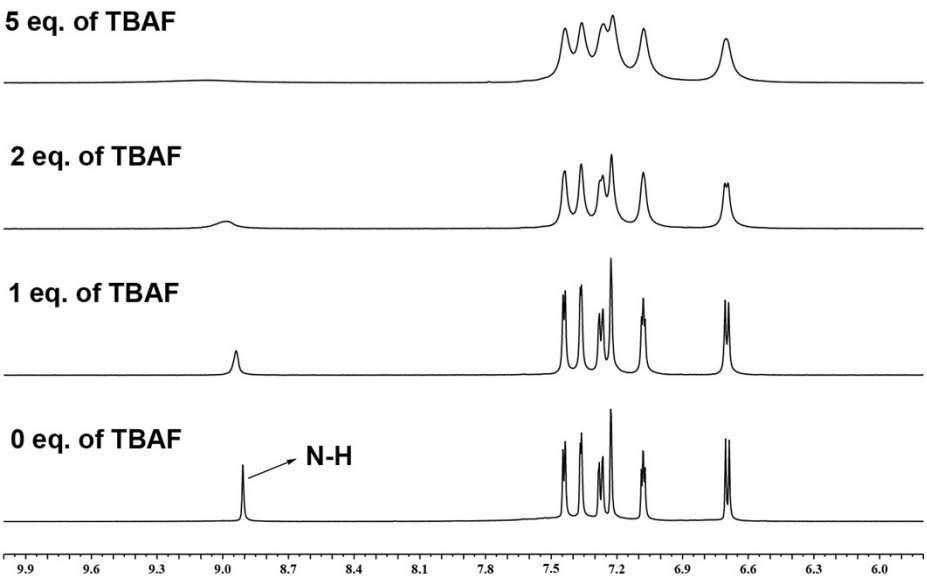

Figure S14 ^{1}H NMR spectra of a mixture of **3a** after addition of 1, 2 and 5 equivs of TBAF.

7. Determination of the detection limit

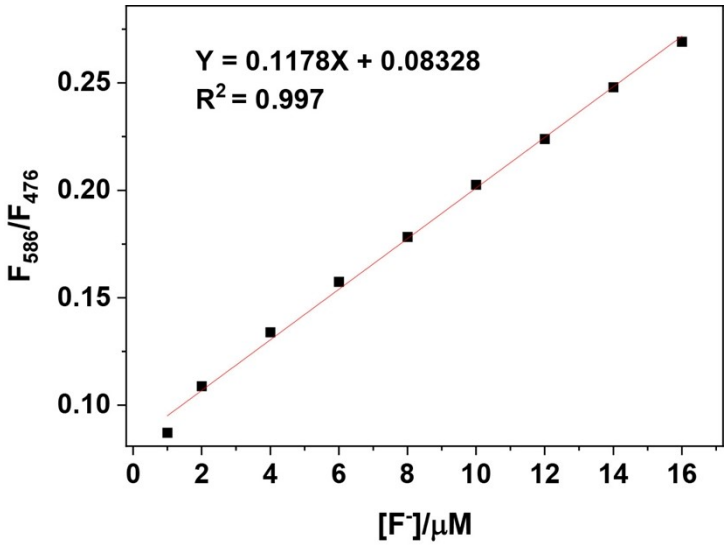

Figure S15. The calibration curves and linear equation of **3a** for FL intensity ratio changes (F_{586}/F_{476}) upon gradual addition of F^-.

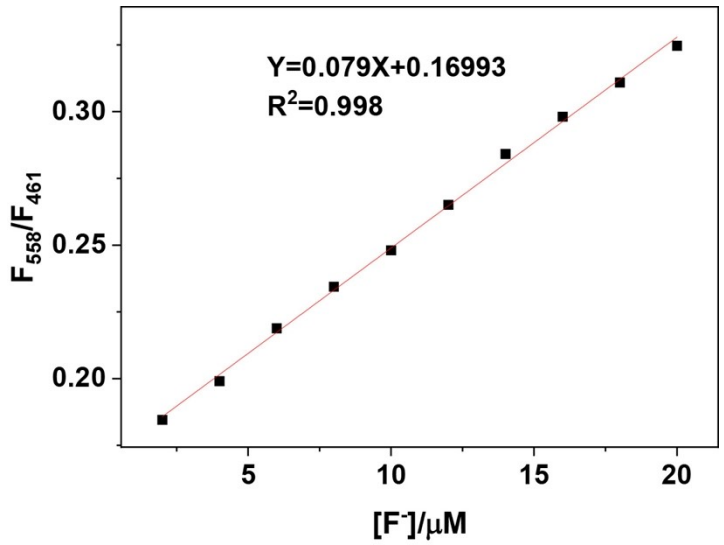

Figure S16. The calibration curves and linear equation of **3b** for FL intensity ratio changes (F_{558}/F_{461}) upon gradual addition of F^-.

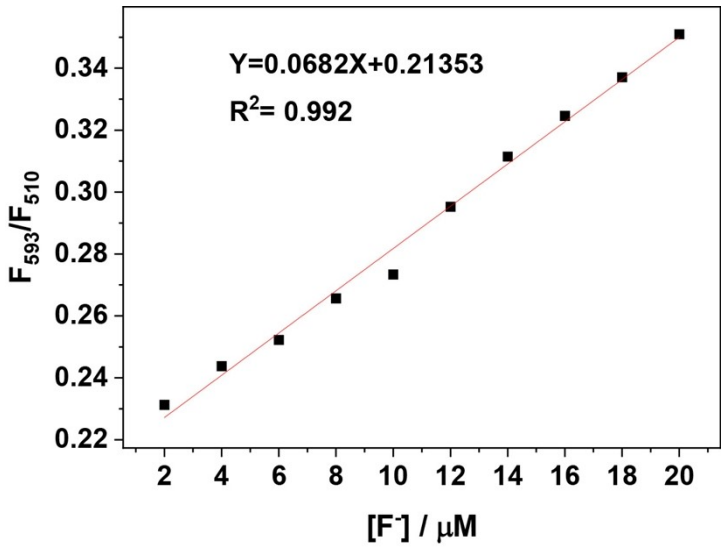

Figure S17. The calibration curves and linear equation of **3c** for FL intensity ratio changes (F_{593}/F_{510}) upon gradual addition of F^-.

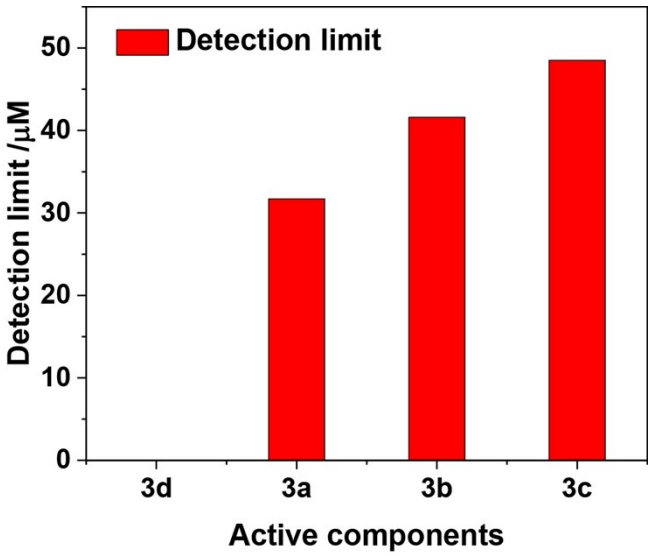

Figure S18. The calculated detection limits of **3a**, **3b**, and **3c**.

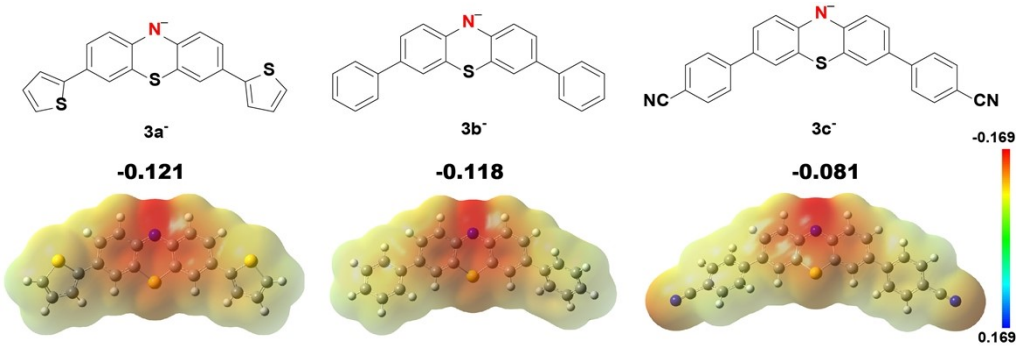

Figure S19. The electrostatic potential mapping of isolated **3a**$^{-}$, **3b**$^{-}$ and **3c**$^{-}$ at the (TD-DFT, B3LYP-D3/6-311+g(d,p)).

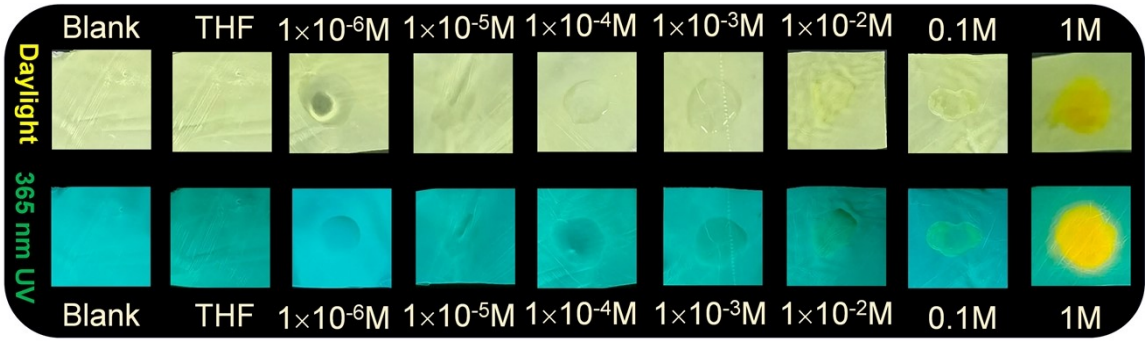

Figure S20. The **3a**-based film for F^{-} detection under daylight (up) and 365 nm UV irradiation (down).

8. Complexation of 3b and 3c with different anions.

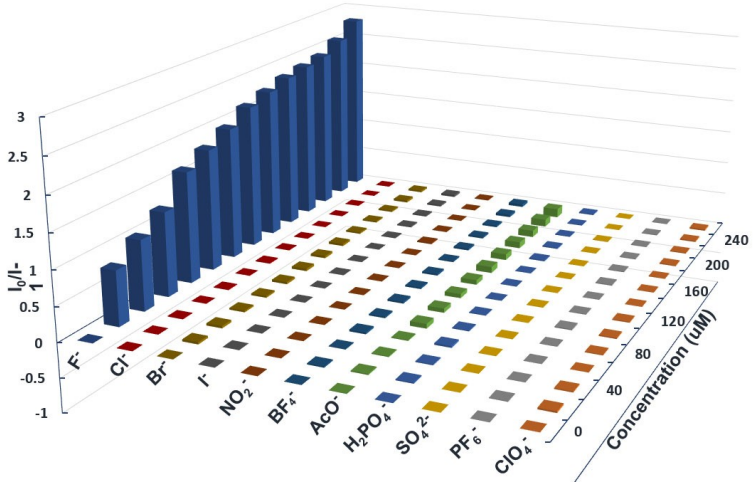

Figure S21. (I_0/I)-1 of F^- and other anions for the emission of **3b** in THF (10 μM) at different equivalents of anions.

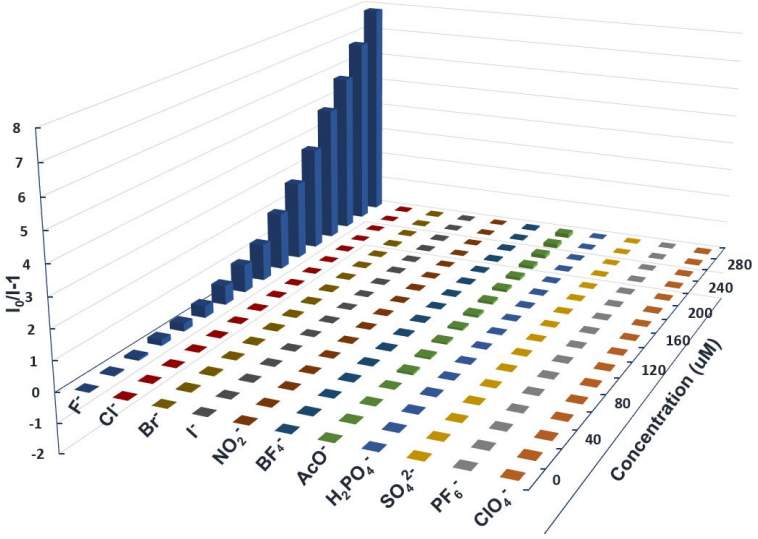

Figure S22. (I_0/I)-1 of F^- and other anions for the emission of **3c** in THF (10 μM) at different equivalents of anions.

9. Hypothesis of electron-transfer mechanism in ECDs

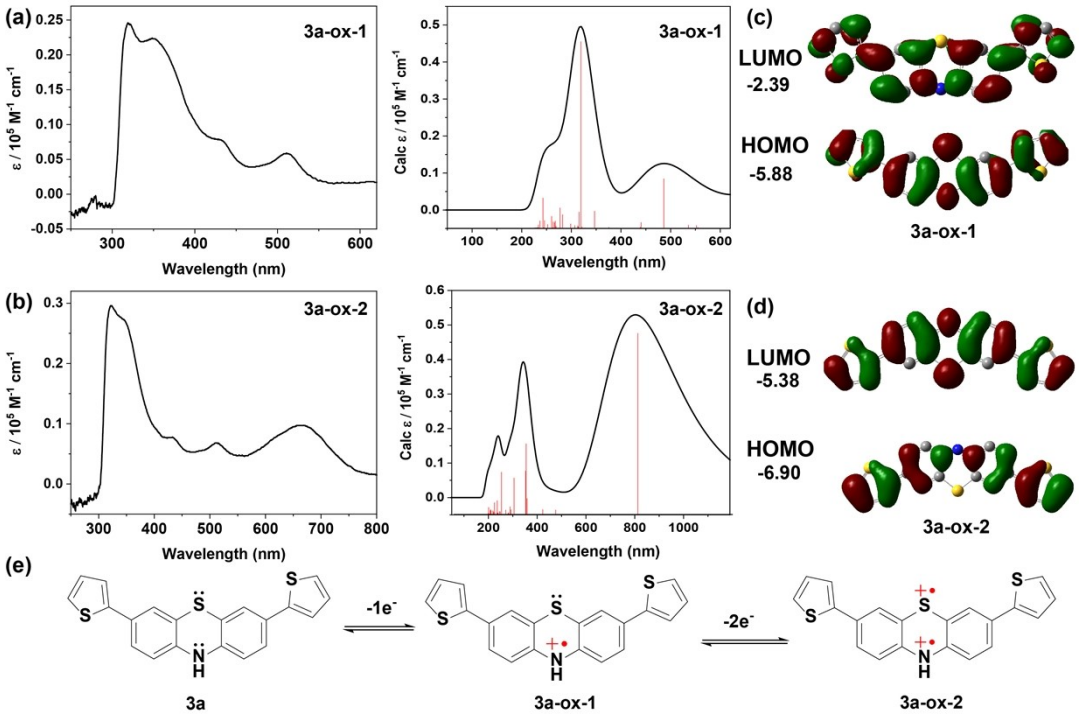

Figure S23 (a) and (b) Experimental and calculated UV-Vis spectra of oxidation states at the TD-DFT, B3LYP-D3/6-311+g(d,p) level of theory; (c) Proposed mechanism for electrochromism of **3a**; (d) HOMO/LUMO orbital plots of oxidation states.

10. optical stability test for electrochromic switching of 3a, 3b, 3c and 3d.

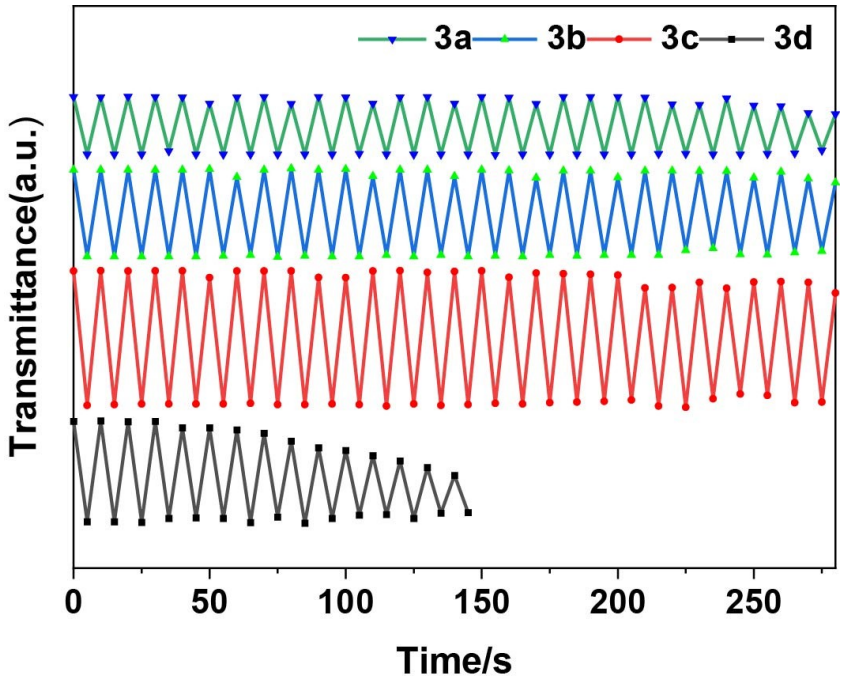

Figure S24. Optical stability test for electrochromic switching of **3a, 3b, 3c** and **3d.**

11. ^{1}H NMR and ^{13}C NMR spectra

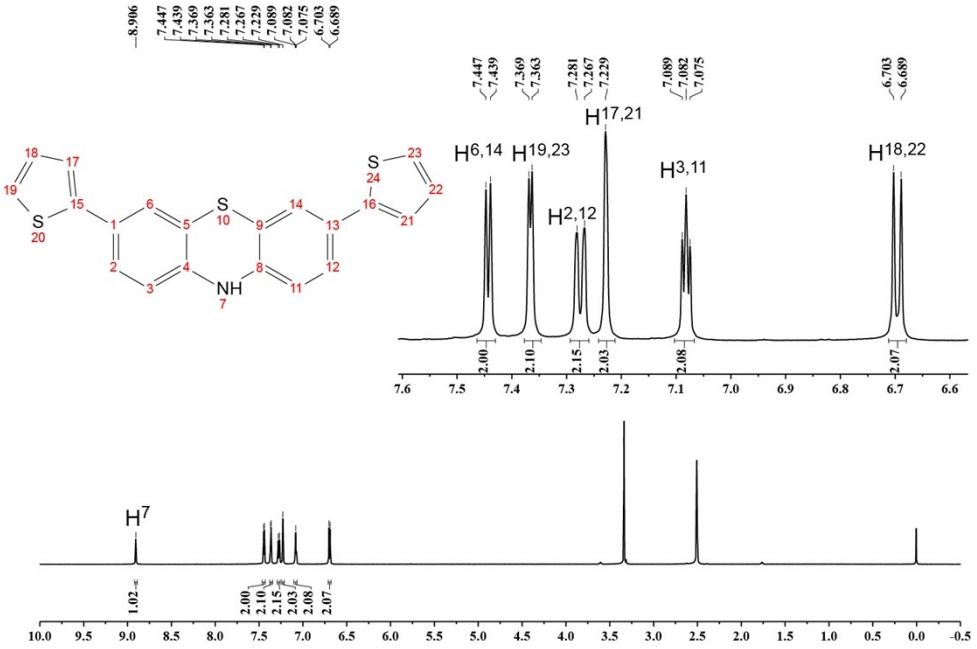

Figure S25. ^{1}H NMR spectrum of **3a** in DMSO

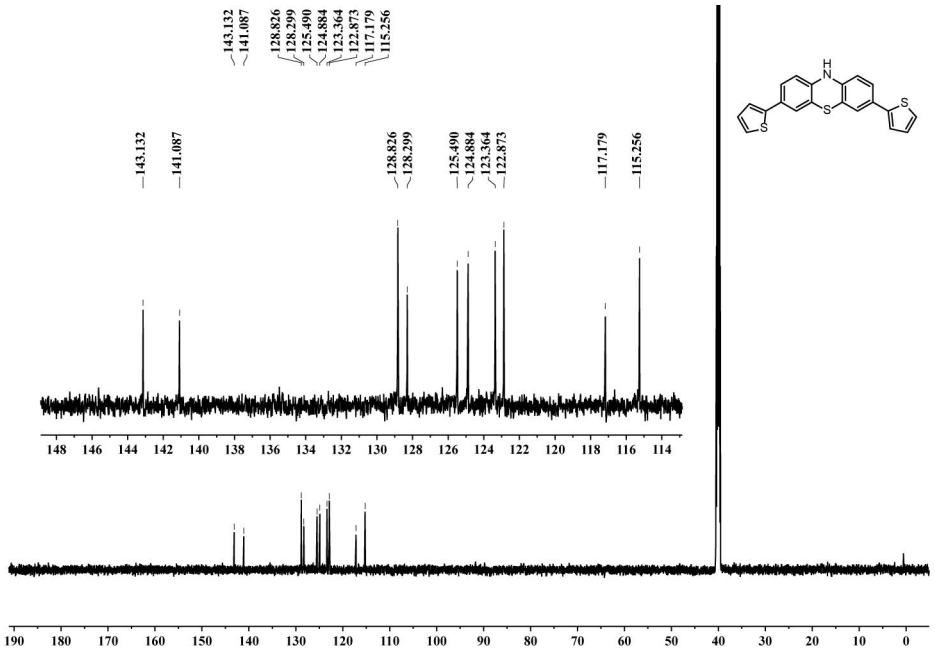

Figure S26. ^{13}C NMR spectrum of **3a** in DMSO

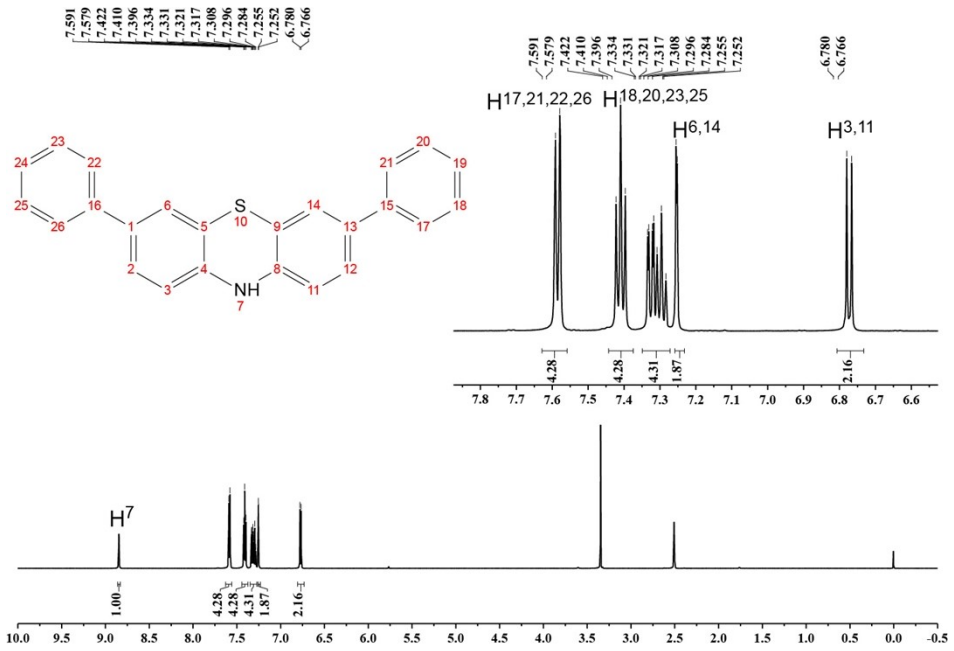

Figure S27. ^{1}H NMR spectrum of **3b** in DMSO

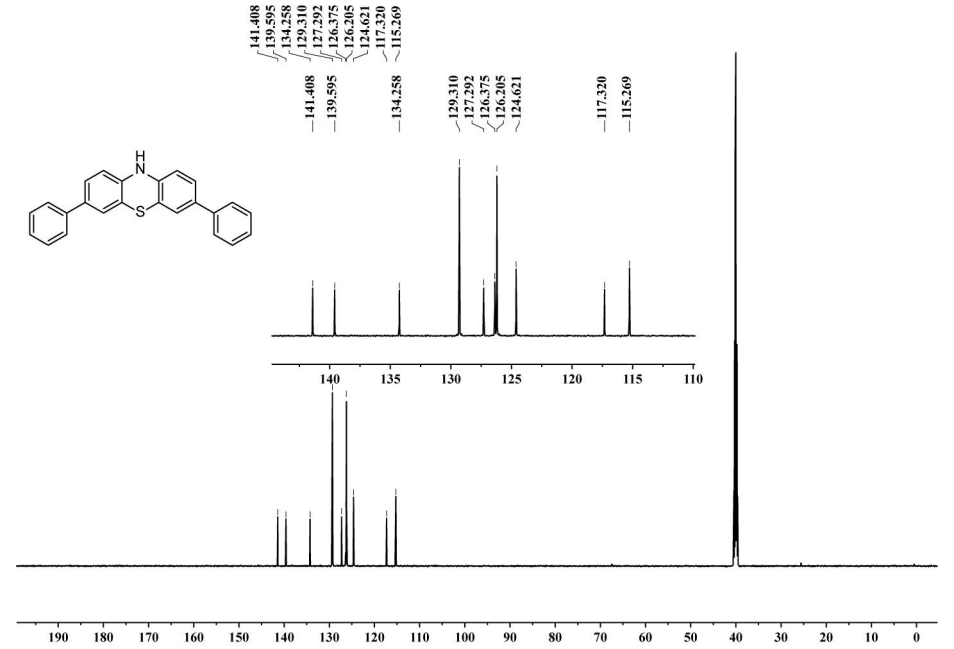

Figure S28. ^{13}C NMR spectrum of **3b** in DMSO

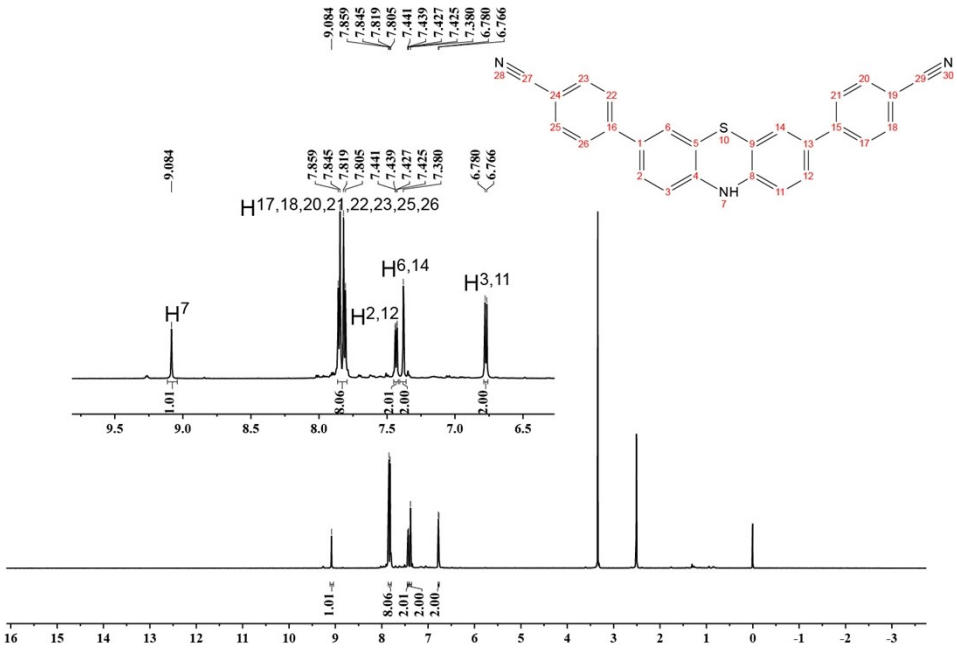

Figure S29. ^{1}H NMR spectrum of **3c** in DMSO

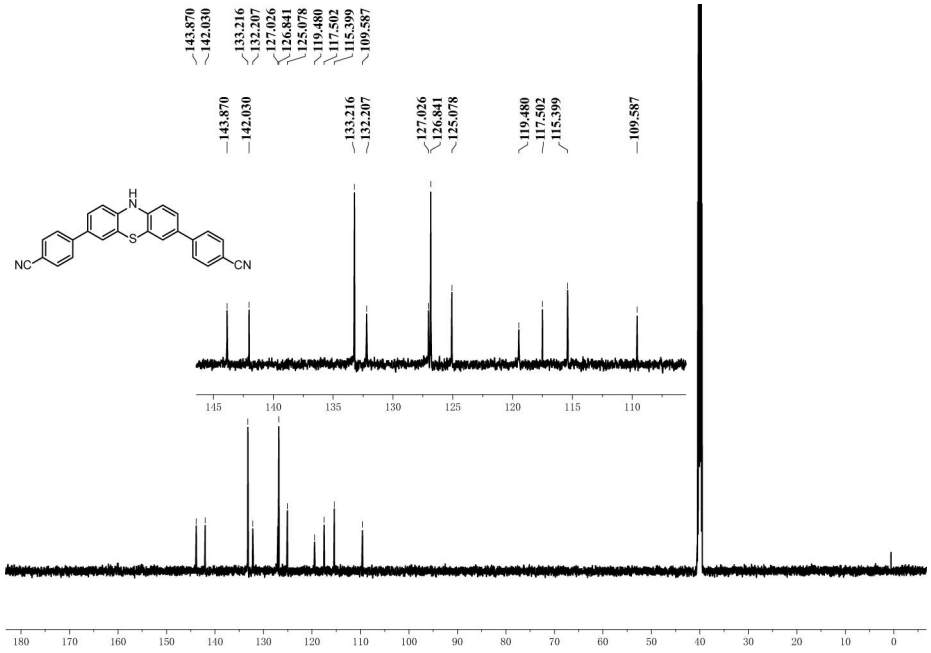

Figure S30 ^{13}C NMR spectrum of **3c** in DMSO

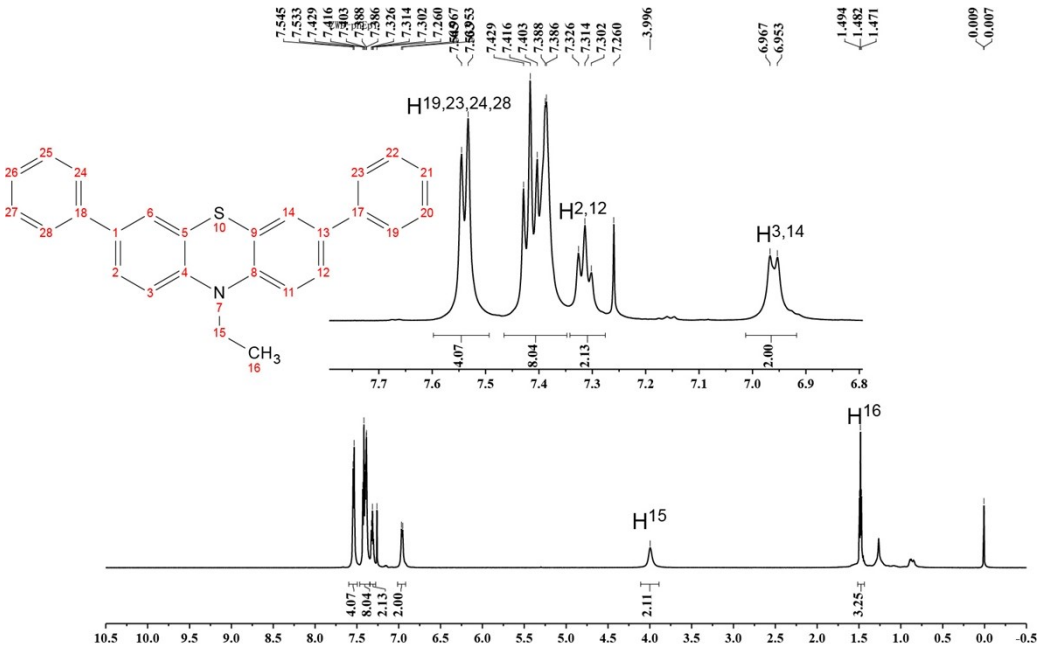

Figure S31. ^{1}H NMR spectrum of **3d** in $CDCl_3$

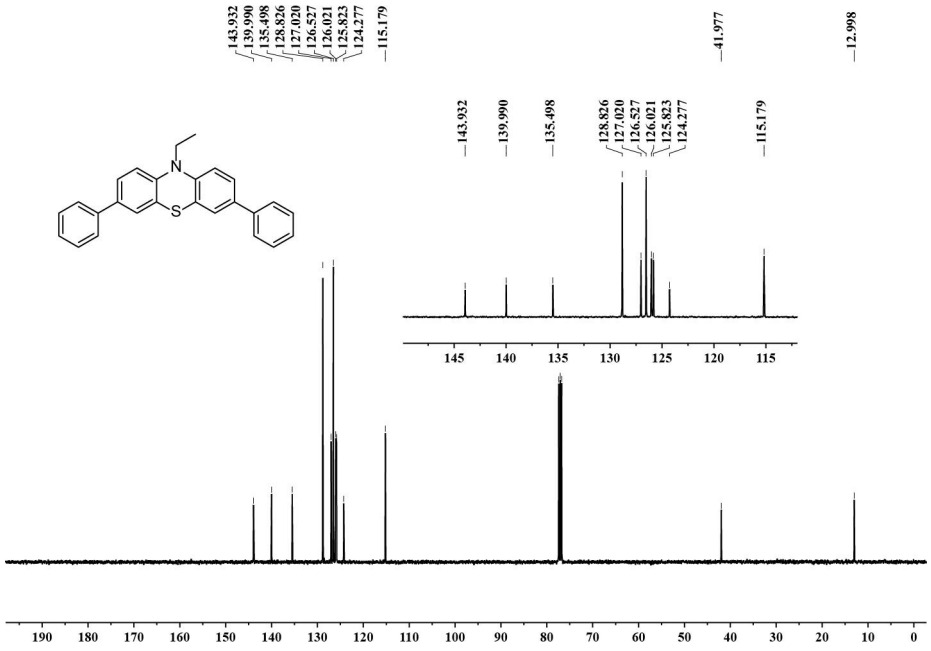

Figure S32. ^{13}C NMR spectrum of **3d** in $CDCl_3$

12. Reference

(1) Miertusˇ, S.; Scrocco, E.; Tomasi, J. *Chem. Phys.* **1981**, *55*, 117.

(2) Cammi, R.; Tomasi, J. J. *Comput. Chem.* **1995**, *16*, 1449.

(3) Tomasi, J.; Persico, M. *Chem. Rev*. **1994**, *94*, 2027.

(4) Cramer,C. J.; Truhlar, D. G. *Chem. Rev*. **1999**, *99*, 2161.

(5) Frisch, M. J.; Trucks, G. W.; Schlegel, H. B. Gaussian09, Revision A.01, Gaussian, Wallingford, Con, USA, **2009**.

Author Contributions

Weidong Zhang conceived the idea for the study. Weidong Zhang prepared the samples and conducted characterizations. Xiucun Feng, Qiangqiang Jia, and Xingliang Liu helped to prepare and characterize the samples. Chao Zhang contributed to the calculations. Weidong Zhang and Kun Zhou wrote the manuscript and all the authors revised and polished the manuscript.